38th International Electric Vehicle Symposium and Exhibition (EVS38) Göteborg, Sweden, June 15-18, 2025

An Error Compensation Method for Enhanced Obstacle Detection in Autonomous Driving

Po-Hua Lee[1], Pin-Yung Chen[1, *], Jinn-Feng Jiang[2],

Tai-Chang Chen[2], Hao-Chu Lin[3]

[1] *Department of Vehicle Engineering of National Pingtung University of Science and Technology, Taiwan, kelvin_chen@mail.npust.edu.tw*

[2] *Metal Industries Research and Development Centre, Taiwan.*

[3]*Department of Marketing and Supply Chain Management of Overseas Chinese University, Taiwan.*

Abstract

The primary objective of this study is to propose an error compensation method for millimeter-wave (mmWave) radar aimed at improving the accuracy of obstacle distance detection in road environments. The proposed approach enhances the reliability of braking decisions by generating high-confidence data, thereby contributing to the safety of passengers and other road users. By employing a straightforward yet effective compensation strategy, sensor-induced errors can be significantly reduced. Moreover, within the framework of the Sustainable Development Goals (SDGs), the advancement of autonomous vehicle radar sensing technologies aligns with SDG 9: Industry, Innovation, and Infrastructure. In particular, improvements in sensing capabilities support the development of more advanced traffic monitoring and control systems. Experimental results validate that the proposed method enables the implementation of a simple, robust, and effective navigation strategy.

Keywords: Radar, Sensing fusion, Kalman Filter, Radar Cross Section, Autonomous Vehicle.

1 Introductions

Millimeter-wave (mmWave) radar plays a pivotal role in autonomous driving by enabling the accurate detection of moving objects and obstacles in the surrounding environment, thereby ensuring vehicle operational safety [1]. However, measurement errors in distance estimation significantly impact radar accuracy, particularly at short ranges, where their effects become more pronounced [2]. Traditional radar metrology often assumes ideal far-field conditions. However, in near-field scenarios, the radar beam illuminates only a limited portion of the target, and the received echo signals are influenced by local geometric variations, leading to unstable measurement results [3].

Moreover, measurement errors in mmWave radar are strongly correlated with beam characteristics, Radar Cross-Section (RCS) fluctuations, and multiple reflection effects. In near-field conditions, the radar beam propagates as a spherical wave, causing the incident angle to vary with distance, thereby affecting the accuracy of RCS measurements [4,5]. Due to the constrained spatial coverage of the radar beam in near-field environments, multiple reflections and diffraction effects are more pronounced, leading to amplified RCS fluctuations and exacerbated measurement errors. Notably, at very short measurement distances, the polar plot of the reflection coefficient exhibits a distorted spiral pattern with a shifting center, introducing nonlinear phase-to-distance errors that necessitate additional compensation to improve measurement precision [6]. As the measurement distance increases, the spherical wave gradually transitions to a plane wave [7], resulting

in broader beam coverage, stabilized target echoes, and enhanced reliability in distance measurements [8].

To mitigate measurement errors in mmWave radar, extensive research has explored multi-sensor fusion techniques, which substantially improve measurement accuracy. For instance, integrating optical cameras with mmWave radar compensates for the radar's inherent limitations in angular resolution [9], while LiDAR technology enhances depth perception and target localization capabilities [10]. Kalman filtering (KF) is widely employed in multi-sensor data fusion to enhance environmental perception accuracy and suppress measurement noise [11]. The fusion of radar and optical image data further strengthens mmWave radar's object detection capabilities, particularly under adverse weather conditions [12].

Given the critical role of accurate obstacle distance estimation in near-field conditions for preventing potential collisions, this study proposes an error compensation method for mmWave radar to enhance the precision of obstacle distance detection in autonomous driving applications.

2 Integrated Sensor Architecture for Accurate Distance Measurement

This study presents an efficient error compensation method aimed at mitigating distance measurement inaccuracies in sensor-based autonomous driving systems, thereby enhancing environmental perception precision. The proposed approach integrates a real-time correction mechanism to refine distance estimations relative to the vehicle's position, facilitating more precise detection of surrounding vehicles, pedestrians, and obstacles. In addition to assessing the efficacy of the compensation mechanism in improving measurement accuracy, this study also examines its impact on the robustness of autonomous driving decision-making and control systems.

The primary sensing component within the proposed framework is the Continental ARS408-21 long-range mmWave radar, which is utilized for detecting obstacles along the vehicle's driving trajectory. Data transmission between the radar and the embedded system is managed via the VP230 chip, functioning as a Controller Area Network (CAN) bus transceiver. To further enhance data reliability, the system incorporates an MTI-G-710 Xsens Inertial Measurement Unit (IMU), which provides vehicle speed and heading angle information.

Object classification is performed using a ZED stereo camera, while data fusion between the radar and camera enhances the accuracy of object detection and localization, ensuring seamless data integration. Additionally, the system supports integration with a Velodyne VLP-32 LiDAR, which provides high-resolution spatial data that can be visually rendered on the display interface.

For computational processing, this study employs the NVIDIA Jetson AGX as the core computing platform, responsible for receiving sensor data and executing the error compensation algorithm to optimize measurement accuracy. Upon completion of the compensation process, the system outputs the refined data in real time and visualizes all detected objects on the display. The overall experimental framework is illustrated in Figure 1.

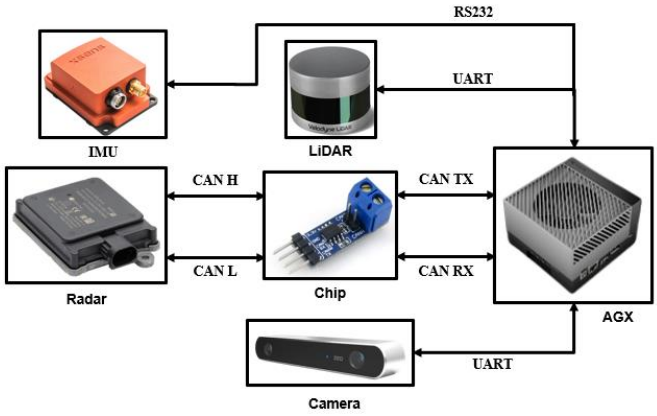

Figure 1: Experimental Framework Configuration

3 Error Compensation Method and Impact Analysis

3.1 Analysis of Radar Error Sources

Millimeter-wave (mmWave) radar is utilized to detect moving objects or obstacles in the surrounding environment, ensuring the safety of the area in front of the vehicle and thereby enhancing the safety of both the vehicle and its occupants. However, the presence of distance measurement errors can affect the radar's accuracy, particularly at short ranges, where these errors become more pronounced. These inaccuracies primarily stem from the radar's beam characteristics, which can introduce significant distance measurement deviations when detecting nearby objects, as illustrated in Figure 2. To mitigate these errors, data fusion and error compensation techniques can significantly improve the accuracy of distance sensing.

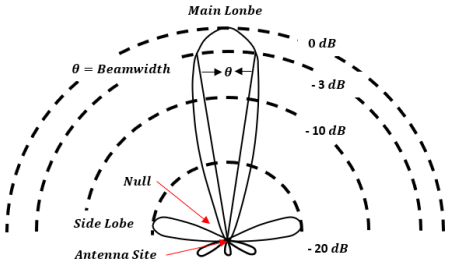

Figure 2: Radiation pattern of a unidirectional antenna

To evaluate and correct these errors, laser rangefinders are typically used in conjunction with mmWave radar to provide accurate data for long-range measurements. Both devices are installed at the same reference point and tested in an open area to minimize environmental interference and ensure measurement accuracy. The testing range typically spans from 5 meters to 70 meters, with measurements taken at intervals of 5 meters. Common road objects, such as pedestrians, motorcycles, and cars, are used as test targets to simulate obstacles encountered in real driving scenarios, further facilitating the analysis and compensation of measurement errors.

The beam characteristics of millimeter-wave radar are the primary cause of significant errors in short-range measurements. According to the radar equation in Eq. (1).

$$P_r = \frac{P_t G_t G_r \lambda^2 \sigma}{(4\pi)^3 R^4} \tag{1}$$

where P_r is the received power, P_t is the transmitted power, G_t and G_r are the transmit and receive antenna gains, respectively, λ is the radar wavelength, σ is the radar cross-section, R is the target distance.

From Eq. (1), it can be observed that as the target distance decreases, the received power increases, and signals from different reflection paths may become stronger. This can affect the interpretation of the echo signal, leading to erroneous calculations of the target distance. Thus, a critical factor influencing the radar measurement accuracy is the antenna's beamwidth and angular resolution.

The angular resolution of a mmWave radar is given by Eq. (2),

$$\theta_{\text{res}} = \frac{\lambda}{D} \tag{2}$$

Where D is the antenna aperture. A larger antenna aperture can reduce the beamwidth, thereby improving angular resolution. As the target approaches, the received power increases; however, this also leads to an

increase in measurement errors. To achieve better angular resolution, a narrower beamwidth is typically required. However, at short distances, the beam spreads more rapidly, and some of the echo signals may not be effectively captured by the receiving antenna, further impacting measurement accuracy. Consequently, mmWave radar operating at short ranges typically exhibits larger distance measurement errors.

3.2 Impact of RCS Measurement on Target Identification Accuracy

During mmWave radar measurements, different targets may introduce varying degrees of error. Therefore, to classify targets, the RCS is commonly used as an indicator. RCS serves as a measure of the target's ability to reflect radar waves, reflecting the target's shape, size, material, and surface characteristics. However, RCS exhibits varying performance at different measurement distances, particularly at short ranges, which can affect the accuracy of target classification.

There is a significant difference in the RCS between the near-field and far-field regions. In the near-field, the radar beam only covers a small portion of the target, and the reflection signals fluctuate due to local geometric variations. Since the incident wave is a spherical wave (rather than a plane wave), the curvature of the wavefront introduces phase differences, which affect the accuracy of RCS measurements. Additionally, due to the limited coverage of the beam, multiple reflections and diffraction effects may occur, further amplifying the RCS fluctuations. As the target distance increases, the spherical wave gradually approximates a plane wave, the radar beam's coverage expands, and reflections from multiple regions of the target are allowed. This broader coverage reduces the impact of local geometric features and diffraction effects, resulting in more stable RCS measurements.

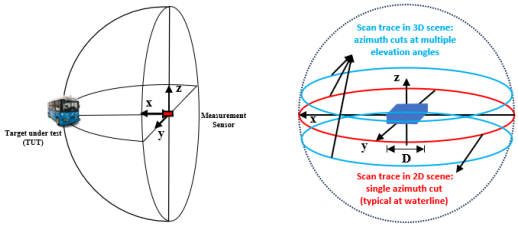

Figure 3: Near-Field Diffraction Effects in Radar Measurements

The beamwidth and its corresponding coverage area play a crucial role in RCS behavior. The beam coverage area can be described by the Eq. (3).

$$R_b = 2R \cdot \tan\left(\frac{\theta_b}{2}\right) \tag{3}$$

Where R represents the distance between the radar and the target, and θ_b is the beamwidth of the radar antenna. As R increases, the beam coverage expands, leading to more stable RCS variations. However, if the beamwidth is excessively large, the radar may lose its ability to distinguish between closely spaced targets, thereby affecting resolution and classification accuracy.

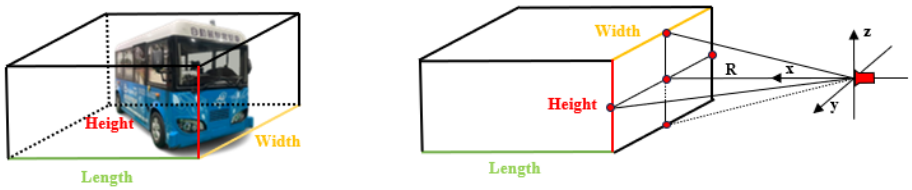

Figure 4: Far-Field Radar Beam Covering a Vehicle

The intensity of the RCS can be determined using a simplified formula based on the received power and transmitted power, as shown in equation (4).

$$\sigma = \frac{P_i}{P_r} \cdot R^2 \tag{4}$$

Where P_i is the transmitted power, P_r is the received power, and R is the distance between the radar and the target. This formula highlights the relationship between RCS, radar-target distance, and the ratio of transmitted to received power.

To facilitate comparisons between different targets, the RCS is typically expressed in decibels relative to one square meter (dBsm). The conversion formula is provided in Eq. (5).

$$RCS_{dBsm} = 10 \log_{10}(\sigma) \tag{5}$$

By analyzing the size of the RCS and its relationship with variations in observation angle and frequency response, different types of targets can be classified. This information also contributes to identifying the shape and structural characteristics of moving objects, thereby enhancing radar-based classification and target recognition capabilities.

3.3 Enhancing Measurement Accuracy and System Stability

To further reduce uncertainties caused by noise or measurement errors, a Kalman filter was incorporated into the compensation process to filter the measurement data, thereby minimizing errors and effectively predicting the future position of the target. The fundamental principle of the Kalman filter lies in state estimation, where the estimated position of the target is dynamically updated by combining the system's dynamic model with the measurement model.

The Kalman filter formula can be expressed as Eq. (6) and (7),

$$\hat{x}_k^- = A\hat{x}_{k-1} + Bu_{k-1} \tag{6}$$

$$P_k^- = AP_{k-1}A^T + Q \tag{7}$$

Where $\hat{x}_k$ is the current state estimate, A is the state transition matrix, B is the control matrix, u is the control vector, P_k is the covariance matrix, Q is the process noise covariance matrix.

The Kalman filter comprises two primary stages: prediction and correction. In the prediction stage, the current state and its associated uncertainty are estimated based on the previous state and the system's dynamic model. However, due to idealized assumptions, external disturbances, and sensor noise, the predicted results may deviate significantly from the actual values. To address this issue, the correction stage incorporates real measurement data to adjust the predicted state. By calculating the Kalman gain, the filter dynamically balances the reliability between the prediction and the measurement, enabling the fusion of both sources of information to refine the state estimate and update its uncertainty. This mechanism effectively reduces estimation errors in real time and enhances accuracy, allowing the system to maintain stable and reliable performance even in noisy and dynamically changing environments. The correction equations are given in Eq. (8)~(10).

$$K = \frac{P_k^- H^T}{HP_k^- H^T + R} \tag{8}$$

$$\hat{x}_k = \hat{x}_k^- + K(z_k - H\hat{x}_k^-) \tag{9}$$

$$P_k = P_k^-(I - KH) \tag{10}$$

Where K is the Kalman gain, H is the measurement matrix, R is the measurement noise covariance matrix, z_k is the actual measurement value, I is the identity matrix.

By incorporating a Kalman filter, accurate target position estimation can be achieved even in the near-field region, where the influence of the target's geometric shape on the measurements is more pronounced. The filter effectively mitigates interference and performs error compensation based on previous estimations and current measurements. This not only enhances the overall measurement accuracy but also improves the reliability of the system. As a result, the system can maintain stability and precision in dynamic environments. The simulation results are shown in Figure 5.

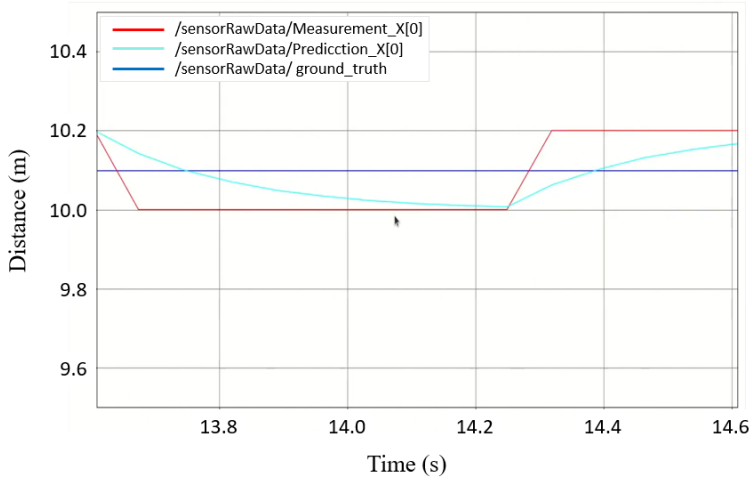

Figure 5: Simulation Results of Kalman Filter-Based Error Compensation

4 Experimental Results

Based on the results of on-road object measurements using the minibus shown in Figure 4, an error of approximately 0.2 meters was detected. This error served as the basis for determining the compensation value required to correct the measurement inaccuracy. The observed measurement errors are closely related to the radar's performance in both the near-field and far-field regions, as illustrated in Figure 6.

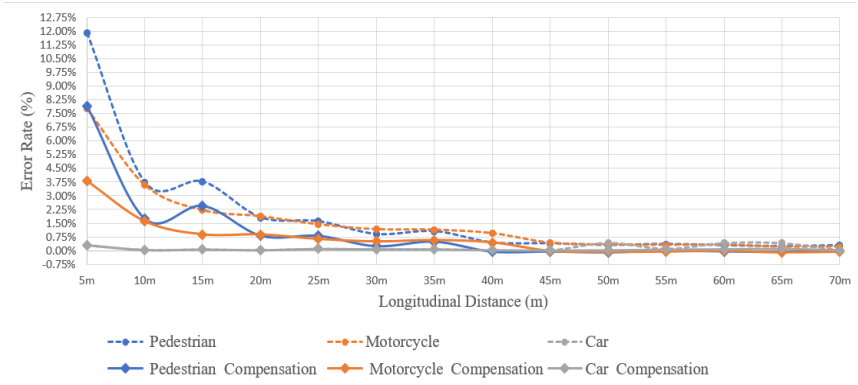

Figure 6: Experimental Results of on-load Driving

In the near-field region, the radar beam covers a relatively smaller area, making the reflected signals more susceptible to the local geometric features of the target. This results in reduced recognition accuracy and increased measurement errors. Under such conditions, precise error detection techniques can be employed to quantify the specific measurement deviation. For instance, in the case of pedestrian detection, an error of 0.2 meters was identified. By subtracting this error from the measured results, the detection accuracy of the system can be significantly improved.

As the target distance increases and the radar transitions into the far-field region, the beam coverage expands and the reflected signals originate from a broader area of the target. This reduces the influence of local geometrical variations and stabilizes the radar cross-section (RCS), thereby greatly enhancing the reliability of target identification in the far-field.

To further improve measurement accuracy, image-based detection techniques were employed in the near-field during the experimental process (as shown in Figure 7), enabling more precise identification of object contours and features. In contrast, RCS-based classification and recognition were applied in the far-field. By integrating these two approaches, the system demonstrates robust recognition capability across varying distance ranges.

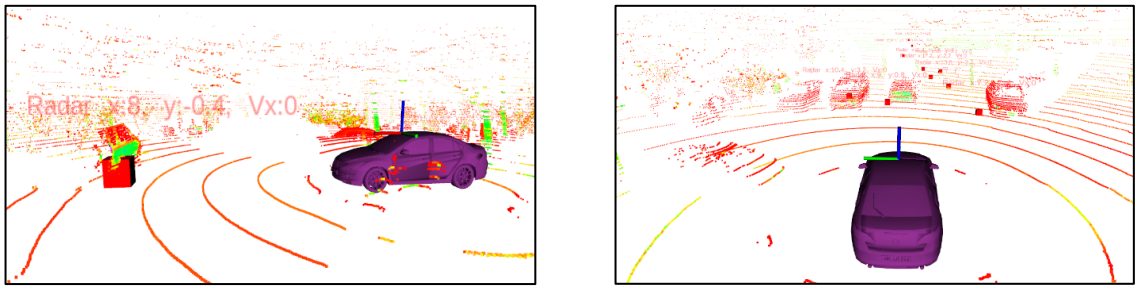

(a) Side View (b) Front View

Figure 7: Sensor Fusion with Camera

5 Conclusions

In this study, a simple distance compensation method was implemented, resulting in a 2.68% reduction in the average error rate. The most significant improvements were observed in the detection accuracy of pedestrians and motorcycles. Although the compensation technique effectively mitigates measurement errors, near-field effects such as radar beam divergence and variations in the target scattering mechanisms—can still lead to increased measurement inaccuracies, particularly for highly scattering targets like pedestrians or non-rigid bodies.

Furthermore, in the near-field region, the curvature of the spherical wavefront induces phase variations, which further exacerbate ranging errors. These errors remain difficult to fully compensate.

As the target distance increases, the radar beam gradually converges, reducing the beam cross-section and enhancing the quality of the reflected signals, thereby improving detection accuracy. Additionally, as the wavefront transitions from spherical to planar with increasing distance, phase variations become more stable, further decreasing ranging errors. Nevertheless, at close range, the divergence of the radar beam continues to impact measurement stability, leading to larger deviations. A comparison of pre- and post-compensation data indicates a marked improvement in longitudinal distance measurement stability at greater ranges.

In addition to optimizing the radar system, integrating LiDAR through sensor fusion presents a promising direction for future development. LiDAR provides high-resolution three-dimensional spatial data, and when fused with radar measurements, it significantly enhances the perception capabilities of autonomous vehicles. This sensor fusion not only improves distance measurement accuracy but also strengthens object recognition reliability, particularly in complex environments with dynamic obstacles.

Acknowledgments

The authors would like to thank the National Pingtung University of Science and Technology of Taiwan and Metal Industries Research and Development Centre for Resource support.

References

[1] U. S. Jha, 2018, The millimeter Wave (mmWave) radar characterization, testing, verification challenges and opportunities, in *Proc. IEEE Autotestcon*, National Harbor, MD, USA, pp. 1–5.

[2] L. Piotrowsky and N. Pohl, 2024, Considerations on Near-Field Correction: µm Accuracy with mmWave Radar, presented at the *IEEE/MTT-S International Microwave Symposium (IMS)*, Washington, DC, USA.

[3] Y. Xie, B. Ning, L. Li, and Z. Chen, 2023, Near-Field Beam Training in THz Communications: The Merits of Uniform Circular Array, *IEEE Wireless Communications Letters*, Vol. 12, No. 4, pp. 575–579.

[4] K. Tsujimura and H. Mori. 2023, Near-Field/Far-Field Transformation for Estimating Direction of Arrival with Bistatic MIMO Radar. *IEEE Radar Conference (RadarConf23)*, San Antonio, TX, USA.

[5] Y. Li, Y. Liu, Y. Wang, Y. Lin, and W. Shen, 2020, The Millimeter-Wave Radar SLAM Assisted by the RCS Feature of the Target and IMU, *Sensors*, Vol. 20, No. 21, pp. 5421.

[6] A. Baskakova and K. Hoffmann, 2019, Investigation of Waveguide Sensors for Ultra-Short-Distance Measurements, *93rd ARFTG Microwave Measurement Conference (ARFTG)*, Boston, MA, USA.

[7] Y. Liu, W. Hu, W. Zhang, J. Sun, B. Xing, and L. Ligthart, 2020, Radar Cross Section Near-Field to Far-Field Prediction for Isotropic-Point Scattering Target Based on Regression Estimation, *Sensors*, Vol. 20, No. 21, pp. 6023.

[8] W. Zhang, X. Zhang, J. Shi, S. Wei and T. Zeng, 2023, Near-Field SAR Image Restoration Framework Via Deep Learning, *IGARSS 2023 IEEE International Geoscience and Remote Sensing Symposium*, Pasadena, CA, USA.

[9] Z. Deng, Z. Cui and Z. Cao, 2022, Super Resolution Detection Method of Moving Object based on Optical Image Fusion with MMW Radar. *IGARSS 2022 IEEE International Geoscience and Remote Sensing Symposium*, Kuala Lumpur, Malaysia.

[10] Y. Zhou, Y. Dong, F. Hou, and J. Wu, 2022, Review on Millimeter-Wave Radar and Camera Fusion Technology, *Sustainability*, Vol. 14, No. 9, pp. 5114.

[11] J. Shi, Y. Tang, J. Gao, C. Piao, and Z. Wang, 2023, Multitarget-Tracking Method Based on the Fusion of Millimeter-Wave Radar and LiDAR Sensor Information for Autonomous Vehicles, *Sensors*, Vol. 23, No. 15, pp. 6920.

[12] D. Xu, Y. Liu, Q. Wang, L. Wang, and R. Liu, 2022, Target Detection Based on Improved Hausdorff Distance Matching Algorithm for Millimeter-Wave Radar and Video Fusion, *Sensors*, Vol. 22, No. 12, pp. 4562.

Presenter Biography

Po- Hua Lee Graduate Student
He received the B. S. degree in Vehicle Engineering from National Pingtung University of Science and Technology, Taiwan, in 2024. He is currently pursuing a Master's degree program in the Department of Vehicle Engineering.

Pin-Yung Chen, Assistant Professor
Pin-Yung Chen received his Ph.D. degree in the Department of Power Mechanical Engineering from the National Tsing Hua University, Hsinchu, Taiwan, in 2018. Before 2023, Dr. Chen was been a senior researcher at the Industrial Technology Research Institute(ITRI), Hsinchu, Taiwan. Currently, Dr. Chen is presently an assistant professor in the Department of Vehicle Engineering, National Pingtung University of Science and Technology, Pingtung, Taiwan. His research interests are intelligent vehicles and autonomouscontrol systems. Dr. Chen is a member of the IEEE Control Systems, Chinese Institute of Engineers Society of Taiwan, Intelligent Transportation Society (ITS) of Taiwan, and SAE Taipei Section.

Jinn-Feng Jiang, Deputy Director
Jinn-Feng Jiang received his Ph.D. degree in the Department of Mechanical Engineering from the National Taiwan University of Science and Technology. With many years of dedicated service in Taiwan's automotive industry, possesses extensive experience in automotive industry R&D. Also served as a research scientist in the DoIT of MOEA, and played a crucial role in advancing Taiwan's smart EV industry and facilitating the production of Taiwan's brand, Luxgen. Recently focusing on the research and promotion of autonomous vehicles and wire-controlled chassis vehicle technology.

Hui-Ting Liang, Manager
Liang Hui-Ting received her master’s degree in Management from National Cheng Kung University. With several years of experience in research and management in the automotive industry, her primary research area focuses on product reliability and testing verification. Recently placed an emphasis on the development of testing verification techniques and regulations for industry promotion related to components of electric vehicles, such as suspension, steering, and braking systems.

Hao-Chu Lin, Associate Professor
Hao-Chu Lin received his Ph.D. degree in management science from the National Taiwan University of Science and Technology in 2011. He was working in the Department of Industrial Technology, Ministry of Economic Affairs, for over twenty years. and has participated include Industrial Technology Development Program, Innovative R&D Centers in Taiwan Program, International Cooperation Program, Promotion of the local industries Innovative Technology Applications and Service Program, etc. Currently, he is an associate professor in the department of Marketing & Supply Chain Management of Overseas Chinese University, Taiwan. His research interests include public administration, technology strategy, foresight research management of innovation and ICT application.